Role of the DNase-I-Binding Loop in Dynamic Properties of Actin Filament

Sofia Yu. Khaitlina* and Hanna Strzelecka-Gołaszewska†
*Department of Cell Culture, Institute of Cytology, 194064 St. Petersburg, Russia; and †Department of Muscle Biochemistry, Nencki Institute of Experimental Biology, 02-093 Warsaw, Poland

ABSTRACT Effects of proteolytic modifications of the DNase-I-binding loop (residues 39–51) in subdomain 2 of actin on F-actin dynamics were investigated by measuring the rates of the polymer subunit exchange with the monomer pool at steady state and of ATP hydrolysis associated with it, and by determination of relative rate constants for monomer addition to and dissociation from the polymer ends. Cleavage of actin between Gly-42 and Val-43 by protease ECP32 resulted in enhancement of the turnover rate of polymer subunits by an order of magnitude or more, in contrast to less than a threefold increase produced by subtilisin cleavage between Met-47 and Gly-48. Probing the structure of the modified actins by limited digestion with trypsin revealed a correlation between the increased F-actin dynamics and a change in the conformation of subdomain 2, indicating a more open state of the filament subunits relative to intact F-actin. The cleavage with trypsin and steady-state ATPase were cooperatively inhibited by phalloidin, with half-maximal effects at phalloidin to actin molar ratio of 1:8 and full inhibition at a 1:1 ratio. The results support F-actin models in which only the N-terminal segment of loop 39–51 is involved in monomer-monomer contacts, and suggest a possibility of regulation of actin dynamics in the cell through allosteric effects on this segment of the actin polypeptide chain.

INTRODUCTION

The dynamics of actin filaments is of primary importance for actin functions in the cell. Cell spreading and formation of adhesion sites on a solid substrate is accompanied by microfilament association into myofibril-like arrays, stress fibers, which rapidly disassemble when the cell starts to move in response to surface stimulation (for a review see Byers et al., 1984). Protrusion and crawling movement of motile cells, neurite growth cone motility (reviewed by Stossel, 1993; Small et al., 1996), or extension of the acrosomal process of certain echinoderm spermatozoids (Tilney and Inoue, 1982) are driven by directional polymerization of actin. *Listeria monocytogenes* and other pathogenic bacteria make use of polymerization of actin recruited from the host to propel themselves through the cytoplasm of infected cells (reviewed by Lasa et al., 1998).

Actin dynamics also reveals itself in a steady-state exchange of the filament subunits with the monomer pools. The exchange occurs even in relatively stable filament assemblies, such as stress fibers, which in stationary cells can persist for hours, and in mature myofibrils (reviewed by Jockusch et al., 1986; Littlefield and Fowler, 1998). The most dynamic are the filaments in locomoting cells. Extension of lamellipodia and filopodia, initiated by formation of new filaments at the leading edge of the cell, is supported by continuous net growth of these filaments at their barbed ends facing the cell membrane, while the net depolymerization at the pointed ends directed toward the cell interior provides monomers for their recycling into new filaments (reviewed by Small et al., 1996). This treadmilling mechanism was first observed for actin in vitro (Wegner, 1976). However, the treadmilling rate in vitro has long been regarded too slow to account for lamellipodia protrusion in fast migrating cells or for propulsion of *Listeria*. This discrepancy seems to be resolved by recent studies on nonmuscle actins and on actin-binding proteins that can regulate actin filament turnover (reviewed by Carlier, 1998; Chen et al., 2000).

The treadmilling is based on a vectorial hydrolysis of actin-bound ATP during filament growth that creates a difference in critical concentrations for polymerization at the pointed end, bearing F-ADP subunits, and at the barbed end, carrying newly incorporated F-ATP subunits (reviewed by Carlier, 1989). Nucleotide-dependent allosteric changes that might underlie the difference in the monomer-monomer affinity between ATP-monomers and ADP-monomers have been detected in electron microscopic studies on F-actin (Orlova and Egelman, 1992; Belmont et al., 1999) and in biochemical studies on both G- and F-actin (Frieden and Patane, 1985; Strzelecka-Gołaszewska et al., 1993; Muhlrad et al., 1994; Kim et al., 1995; Moraczewska et al., 1996, 1999). These changes have been localized to subdomain 2 of actin, in particular its surface loop 39–51, known as the DNase-I-binding loop, and to the C-terminal area in subdomain 1. The nucleotide-dependent rearrangement of the DNase-I-binding loop has been confirmed by the most recently reported crystal structure of uncomplexed G-actin in the ADP state (Otterbein et al., 2001).

Atomic models of the actin filament published thus far (Holmes et al., 1990; Lorenz et al., 1993; Tirion et al., 1995) predict that the DNase-I-binding loop is involved in the

Received for publication 3 April 2001 and in final form 9 October 2001.
Address reprint requests to Hanna Strzelecka-Gołaszewska, Department of Muscle Biochemistry, Nencki Institute of Experimental Biology, 3 Pasteur Street, 02-093 Warsaw, Poland. Tel.: 48-22-6686182; Fax: 48-22-8225342; E-mail: hannas@nencki.gov.pl.

0006-3495/02/01/321/14 $2.00

monomer-monomer contacts along the two-start F-actin helix. This prediction is supported by biochemical data showing that chemical or proteolytic modifications of loop 39–51 perturb polymerization of actin (Hegyi et al., 1974; Schwyter et al., 1989; Khaitlina et al., 1991, 1993), and with polymerization-related changes in the fluorescence of dansyl probes on Gln-41 (Takashi, 1988; Kim et al., 1995; Moraczewska et al., 1999). However, the arrangement of this loop in F-actin and, consequently, its contacts has not yet been unequivocally established. The uncertainties arise from the fact that, in monomeric actin, it is the most mobile area of the molecule (McLaughlin et al., 1993), and the crystal structure used to build the F-actin models (Kabsch et al., 1990) shows it in the conformation stabilized by its direct binding to DNase-I. The refined versions of the model (Lorenz et al., 1993; Tirion et al., 1995) improved the fit to electron microscopic three-dimensional reconstructions of F-actin by shifting subdomain 2 (or subdomains 1 and 2) toward the filament axis and by a rearrangement of loop 39–51. Different modes of the refinement resulted in a strikingly different orientation of this loop and different number of its intermonomer interactions in the two models (Ben-Avraham and Tirion, 1995). One should also mention that the models are based on x-ray fiber diffraction patterns from F-actin gels stabilized by phalloidin, and the conformation of loop 39–51 as well as the orientation of the whole subdomain 2 in the polymer are strongly influenced by this toxin (Lorenz et al., 1993; Orlova et al., 1995).

We have previously shown that proteolytic cleavage of loop 39–51 between residues 42 and 43 (Khaitlina et al., 1991, 1993) has a stronger inhibitory effect on polymerization of actin than the cleavage of the same loop between residues 47 and 48 (Schwyter et al., 1989). Here we have investigated the dynamic properties of the filaments assembled from such modified actins. The rates of the polymer subunit exchange with the monomer pool at steady state were examined by measuring the rates of ATP hydrolysis associated with the monomer incorporation into the polymer and, directly, by following incorporation of fluorescently labeled G-actin into non-labeled F-actin. These measurements were supplemented with determination of changes in rate constants for monomer addition to and dissociation from the filament ends. Limited proteolysis with trypsin was used to probe changes in actin structure. The results are discussed in terms of distinct roles of various parts of the DNase-I-binding loop in the monomer-monomer interactions and in the dynamic properties of actin filament.

MATERIALS AND METHODS

Reagents

Trypsin (from bovine pancreas, TPCK-treated), subtilisin (Carlsberg, from *Bacillus licheniformis*), Hepes, dithiothreitol, 1,N^6-etheno-ATP (ϵ-ATP), and ATP were purchased from Sigma Chemical Co. (St. Louis, MO). SDS was from Carl Roth KG Chemische Fabrik (Karlsruhe). *N*-(1-pyrenyl)-iodoacetamide was from Molecular Probes (Eugene, OR). The protease ECP32 from *Escherichia coli* A2 strain was kindly provided by Drs. A. Morozova and A. Malinin (Institute of Cytology, St. Petersburg, Russia). All other reagents used in experiments were of analytical grade.

Protein preparations

Rabbit skeletal muscle actin was prepared according to Spudich and Watt (1971) with additional purification by gel filtration on a Sephadex G-100 column. G-actin was stored in buffer containing 2 mM Hepes, pH 7.6, 0.2 mM ATP, 0.1 mM $CaCl_2$, 0.2 mM dithiothreitol, and 0.02% NaN_3 (buffer G). Actin fluorescently labeled at Cys-374 with *N*-(1-pyrenyl)iodoacetamide was prepared as described previously (Khaitlina et al., 1993). The extent of labeling was determined spectrophotometrically using an absorption coefficient of $2.2 \times 10^4\ M^{-1}\ cm^{-1}$ at 344 nm (Kouyama and Mihashi, 1981). Ca-G-actin was transformed into Mg-G-actin by a 3–5 min incubation with 0.2 mM EGTA/0.1 mM $MgCl_2$ at 25°C. The concentration of G-actin was determined spectrophotometrically using an absorption coefficient of 0.63 mg ml^{-1} at 290 nm (Houk and Ue, 1974). The absorbance values for pyrenyl-labeled actin were corrected for the contribution of the label by subtracting $0.33 \times A_{344}$.

ECP-cleaved actin was obtained using a preparation of *E. coli* protease ECP32 additionally purified to remove a contamination with an ATPase activity (Morozova et al., 2001). Ca-G-actin (2–3 mg/ml) was digested at an enzyme to actin mass ratio of ~1:100, overnight, at 4 μM. Since actin cleaved with protease ECP 32 between Gly-42 and Val-43 is fairly resistant to further digestion with this protease, it was not necessary to use any protease inhibitor. The cleaved actin was used within 10–12 h.

Subtilisin-cleaved actin was prepared as described by Schwyter et al. (1989) except that an enzyme-to-actin mass ratio was 1:1500. The cleavage was followed by one cycle of polymerization-depolymerization.

ATP hydrolysis measurements

Hydrolysis of ATP in G-actin solutions, during polymerization, or in F-actin solutions at steady state was followed by determination of released P_i with the highly sensitive Malachite Green method (Kodama et al., 1986), after quenching the reaction with an equal volume of ice-cold solution of 0.6 M perchloric acid and removal of precipitated protein by centrifugation.

Measurements of the relative number concentration of actin filaments

The relative number concentration of the filaments in solutions of intact and proteolytically modified F-actins was determined by comparing their abilities to nucleate polymerization of G-actin above its critical concentration in polymerizing buffer. We used the assay described by Carlier et al. (1984) with certain modifications. Pyrenyl-labeled (in 9%), 12 μM Mg-G-actins were polymerized with 0.1 M KCl to steady state in the presence of 10 μM Hepes, pH 7.6, and 0.5 mM ATP, at 25°C. Aliquots of these solutions were diluted 24-fold, using truncated Pipetman tips, into 9% pyrenyl-labeled 5 μM ECP-cleaved Mg-G-actin or 3 μM Ca-G-actin supplemented with 0.1 M KCl several seconds before addition of the F-actin seeds. The solutions were mixed in the fluorescence cuvettes by inverting the cuvettes five times. This procedure resulted in a dead time of ~10 s, after which the increase in the pyrenyl fluorescence associated with polymerization of the labeled G-actin (Kouyama and Mihashi, 1981) was recorded at 25°C. The relative number concentration of filaments in F-actin seed solutions is given by the ratio of the rates of filament elongation derived from the slopes of initial linear parts of the fluorescence curves. The filament number in solutions of both cleaved and intact F-actin was

stable from ~60 min to at least 120 min after addition of KCl and, in this time range, it was proportional to the F-actin concentration.

The use of the Ca-form of G-actin was convenient for two reasons. It ensured stability of the G-actin solution during long-lasting experiments and the lag phase in the KCl-induced polymerization long enough to exclude the contribution of spontaneous polymerization to the measured initial elongation rate. For this assay the Ca-G-actin was diluted with a Ca^{2+}-free buffer. Because F-actin-bound divalent cation is virtually unexchangeable, it was assumed that free Ca^{2+} present in the G-actin solution (5–10 μM, with 4 μM $MgCl_2$/8 μM EGTA introduced with F-actin) did not replace the bound Mg^{2+} in F-actin seeds under polymerization conditions of the assay.

Measurements of the relative rate constants for monomer addition to and dissociation from the filament ends

Relative rate constants for monomer addition to (k_+) and dissociation from the filament ends (k_-) were determined from plots of the initial rates of filament elongation on F-actin seeds, or the rates of F-actin depolymerization, versus the monomer concentration, using pyrenyl-labeled actin to monitor the changes in F-actin concentration. The measurements were performed essentially as described by Carlier et al. (1986). The seeds (12 μM, 9% pyrenyl-labeled Mg-F-actins in 0.1 M KCl, 10 mM Hepes, pH 7.6, and 0.5 mM ATP) were diluted into solutions of Mg-G-actin, intact or cleaved, as described above for determination of the relative number concentration of the filaments. Both the polymer elongation and depolymerization were assayed in the presence of 0.1 mM $MgCl_2$, 0.2 mM EGTA, 0.5 mM ATP, and 0.1 M KCl, with G-actins pyrenyl-labeled at the same extent as the F-actin seeds, at 25°C, in the range of G-actin concentrations at which no spontaneous polymerization occurred within the time necessary to measure the initial rate of the nucleated polymerization. The series of the measurements with intact and cleaved G-actins were performed immediately one after another, within 60–90 min after polymerization of the corresponding seed solution, and were started and terminated with determination of the relative number concentration of filaments in the seed solutions as described above. To convert the initial changes in the pyrenyl fluorescence into changes in F-actin concentration, the fluorescence change associated with polymerization to a steady state of 1 μM actin was calculated for each of the assayed actins from the fluorescence increase observed on its polymerization to steady state at the concentration of 12 μM, with F-actin concentration calculated as the difference between the total actin and the critical concentration determined in the same experiment by the elongation assay. Then the rates were normalized to the same number concentration of filaments in the seed solutions, except for the cases when polymerization of different G-actins was nucleated by the same F-actin, either intact or cleaved.

Exchange of the tightly bound nucleotide

The dissociation rates of G-actin-bound nucleotide, which are rate-limiting for the exchange reaction, were determined by displacing the bound ATP with ϵ-ATP added in a high excess over ATP (free and initially bound to actin), so that the rebinding of ATP could be neglected. The concentration of free ATP in G-actin solutions was diminished to 1 μM by passing the protein (2.5–3.5 mg/ml) through a Sephadex G-25 column equilibrated and eluted with buffer G containing ATP at that concentration. The gel-filtered protein was diluted to 5 μM, transformed into Mg^{2+}-bound form by incubation for 3 min with 0.2 mM EGTA/0.1 mM $MgCl_2$, and the exchange reaction was immediately started by addition of 0.1 M ϵ-ATP. Incorporation of ϵ-ATP into G-actin was monitored by measuring an increase in the fluorescence intensity at 410 nm after excitation at 350 nm. Concentration of ϵ-ATP was determined spectrophotometrically using an absorption coefficient of 5700 M^{-1} cm^{-1} at 265 nm (Secrist et al., 1972).

Probing the conformation of actin by limited digestion with trypsin

Digestions with trypsin were performed as described in the figure legends. The proteolysis was stopped with soybean trypsin inhibitor added at a threefold mass excess over trypsin. Digestion products were analyzed by SDS/PAGE performed according to Laemmli (1970) on 12% (mass/vol) gel slabs. Densitometry of Coomassie Blue-stained protein bands was performed in a Shimadzu CS-9000 dual-wavelength flying-spot scanner.

Fluorescence and light-scattering measurements

All fluorescence and light-scattering measurements were performed in a Spex Fluorolog 2 spectrofluorimeter. Fluorescence intensity of pyrenyl-labeled actin was monitored at 407 nm after excitation at 365 nm (Kouyama and Mihashi, 1981). Intensity of light scattered at 90° was measured at 350 nm.

Electron microscopy

Solutions of 24 μM F-actin were diluted 10-fold with an appropriate buffer solution, applied to carbon-coated grids covered with Formvar, and negatively stained with 1% (w/v) uranyl acetate. Specimens were examined in a Joel JEM 1200 EX electron microscope at an accelerating voltage of 80 kV.

RESULTS

Effects of proteolytic cleavages within loop 39–51 on ATP hydrolysis in solutions of F-actin at steady state

Hydrolysis of actin-bound ATP associated with salt-induced polymerization of skeletal muscle actin containing Mg^{2+} at the high-affinity site (Mg-actin) is tightly coupled to the incorporation of the monomers into polymer (Carlier et al., 1987). When polymerization is complete, F-actin continues to hydrolyze free ATP in solution at a constant steady-state rate which, in ionic conditions optimal for polymerization and at temperatures in the range 20–25°C is, however, very low (Asakura and Oosawa, 1960). As shown in Fig. 1, when Mg-actin cleaved between residues 42 and 43 with ECP was polymerized with 0.1 M KCl at 25°C, P_i liberation did not level off after a steady state of polymerization had been reached, but continued with a rate similar to that during the polymer growth.

Fig. 2 shows that cleavage of actin between residues 47 and 48 with subtilisin (Schwyter et al., 1989) influenced ATP hydrolysis in F-actin solutions at steady state much less than cleavage with ECP. The hydrolysis rate increased less than threefold, from 0.038 mol/mol actin/h to 0.10 mol/mol actin/h in the presence of 0.1 M KCl, at 25°C. Under the same conditions, the rate of ATP hydrolysis in solutions of F-actin cleaved with ECP was 4.3 mol/mol actin/h, two orders of magnitude higher than that observed with intact F-actin.

In view of the relatively high critical concentration of ECP-cleaved actin (Khaitlina et al., 1993), one should con-

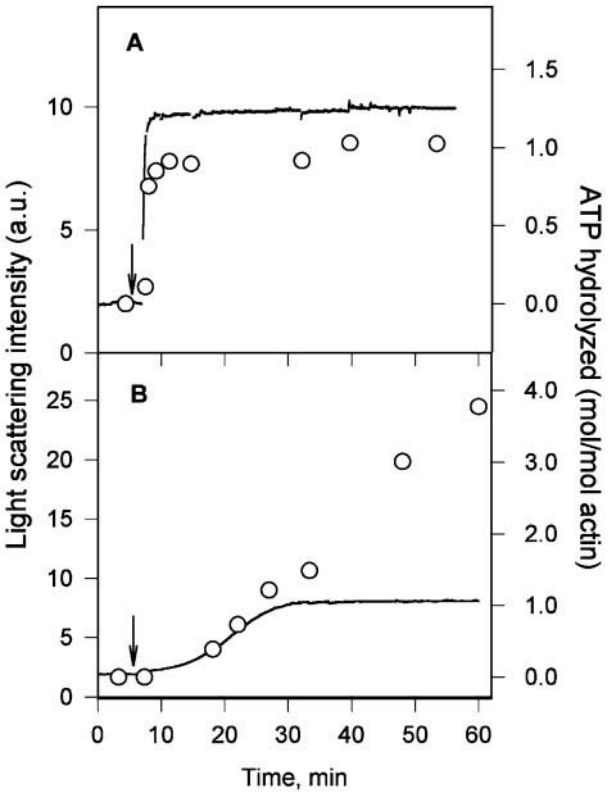

FIGURE 1 Time courses of polymerization of intact and ECP-cleaved actins and of the accompanying ATP hydrolysis. Twenty-four μM intact (*A*) and ECP-cleaved Ca-G-actin (*B*) were transformed into Mg-G-actins as described in Materials and Methods and polymerized by addition of KCl to 0.1 M (*arrow*) at 25°C. Polymerization (*solid traces*) was monitored by recording light-scattering intensity at 350 nm, and P_i concentration (*circles*) was determined in 100-μl aliquots of the solutions taken at time intervals from the cuvette.

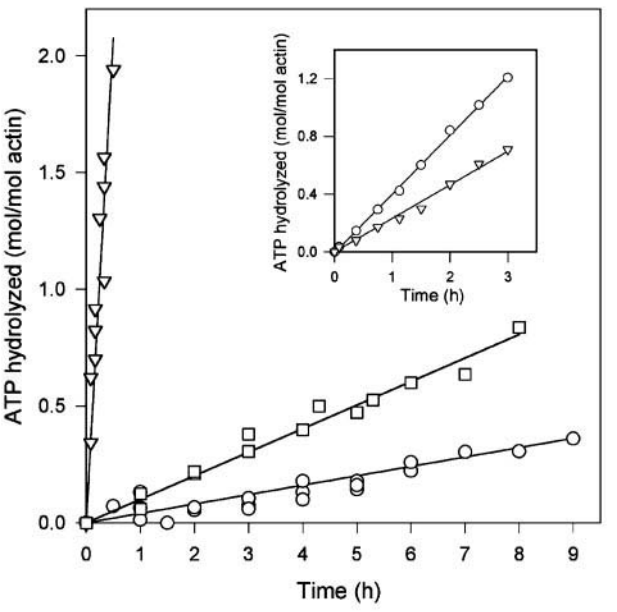

FIGURE 2 Steady-state ATP hydrolysis in solutions of F-actins assembled from intact (*circles*), subtilisin-cleaved (*squares*), and ECP-cleaved G-actin (*triangles*). Mg-G-actins (24 μM) were polymerized with 0.1 M KCl for 30 min and were further incubated at 25°C. At time intervals, aliquots of the solutions were withdrawn for determination of P_i concentration. The concentration of P_i in sample taken first (time 0 in the figure) was subtracted from the values obtained for all other samples. Data for intact and ECP cleaved actins are from three, and those for subtilisin-cleaved actin are from two independent experiments. The inset shows ATP hydrolysis in solutions of 24 μM intact (*circles*) and ECP-cleaved Mg-actin (*triangles*) in the absence of any added salt. Data for ECP-cleaved actin are average values from two independent experiments.

sider a possibility of enhancement of the Mg^{2+}-dependent ATPase activity of G-actin (Brenner and Korn, 1981) as one of the reasons for the high rate of ATP hydrolysis in solutions of cleaved F-actin. This possibility is excluded by data in the inset to Fig. 2, showing that the rate of ATP hydrolysis in Mg-G-actin solutions was slightly diminished rather than increased by cleavage of actin with ECP.

Effects of actin cleavage between residues 42 and 43 on the monomer-polymer subunit exchange at steady state

It is generally believed that the steady-state ATPase activity of F-actin reflects dissociation of ADP-bearing subunits from the filament ends, ADP for ATP exchange on the monomers, and hydrolysis of the bound ATP upon reincorporation of ATP-monomers into filaments. However, an enhancement of the F-actin ATPase under certain conditions, e.g., under sonic vibration or at high temperatures, has been suggested to result from a direct exchange of F-actin-bound ADP for ATP due to a loosening of the F-actin structure under these conditions (for a review see Oosawa, 1983). Experimental evidence for ATP hydrolysis associated with an exchange of F-actin-bound ADP for ATP independent of the monomer dissociation from and reassociation to the polymer ends has been provided by comparing the rates of ATP hydrolysis and of subunit exchange in F-actin under conditions of partial polymerization (Brenner and Korn, 1984).

To elucidate the mechanism of the enhancement of the steady-state ATPase activity of F-actin by actin cleavage between residues 42 and 43, we compared the kinetics of ATP hydrolysis and of actin monomer-polymer subunit exchange in solutions of intact and cleaved F-actin. The rate and final extent of exchange of G-actin with F-actin subunits were measured by the procedure of Brenner and Korn (1983, 1984). Trace amounts of pyrenyl-labeled intact or ECP-cleaved Mg-G-actin were gently mixed with the corresponding non-labeled Mg-F-actins, and an increase in the fluorescence intensity accompanying incorporation of the labeled monomers into F-actin (Kouyama and Mihashi, 1981) was monitored. To prevent self-polymerization of the labeled G-actins, their final concentration was kept at 0.04

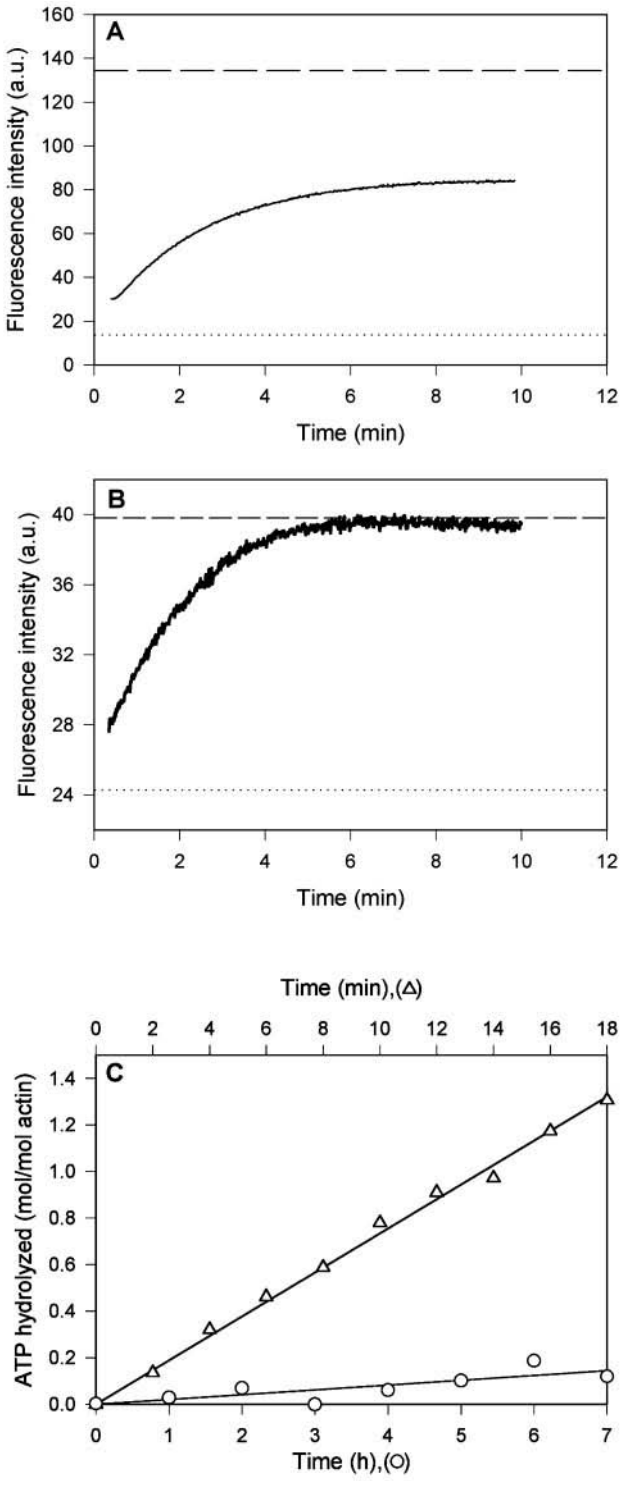

FIGURE 3 Incorporation of intact and ECP-cleaved G-actin into the corresponding F-actin and hydrolysis of ATP at steady state. Intact (*A*) and ECP-cleaved Mg-G-actin (*B*), 12 μM, were polymerized to steady state with 0.1 M KCl in the fluorescence cuvettes at 25°C. Then (time 0 in the figure) pyrenyl-labeled Mg-G-actin (intact or ECP-cleaved, correspondingly) was added at the final concentration of 0.04 μM. The proteins were gently mixed by inversion, and the pyrenyl fluorescence was monitored (*solid traces*). The initial fluorescence (*dotted lines*) was measured in a mixture of 0.04 μM pyrenyl-labeled and 12 μM nonlabeled actin in the absence of salt, and the final fluorescence at equilibrium (*dashed lines*) is the fluorescence of a co-polymer of the labeled and nonlabeled protein. Each curve is an average of two measurements. (*C*) ATP hydrolysis in parallel samples of KCl-polymerized intact (*circles*) and ECP-cleaved actin (*triangles*) supplemented with pyrenyl-G-actin as in (*A*) and (*B*).

μM, that is, below the critical concentration for polymerization of both ECP-cleaved and intact actin under conditions used in our experiments. Steady-state ATP hydrolysis was measured in aliquots taken from the fluorescence cuvette or in parallel samples of non-labeled G-actin copolymerized with labeled G-actin. In both cases P_i was liberated with the same constant rate, indicating that ATP hydrolysis associated with a possible transient increase of the number of filament ends, resulting from filament fragmentation upon mixing F-actin with labeled G-actin, did not significantly contribute to the measured rate. Because the steady-state ATPase of intact F-actin under conditions optimal for polymerization is very low, the measurements of P_i liberation in the solutions of this actin had to be prolonged far beyond the time necessary for equilibration of the fluorescence between the monomer and polymer pool.

Fig. 3 shows that, under identical experimental conditions, the incorporation of the labeled monomers into F-actin occurred faster with cleaved actin than with the intact one. The maximum value of the pyrenyl fluorescence intensity was reached within ~6 and 10 min, respectively. Moreover, the final fluorescence enhancement for intact actin was only 62% of the equilibrium value obtained by determination of the fluorescence intensity of the copolymer of labeled and non-labeled G-actins. With cleaved actin, the fluorescence intensity at the plateau was close to the equilibrium value. As can be seen in Fig. 3, this equilibrium value was substantially lower for cleaved than for intact actin. This difference results from the higher critical concentration of cleaved actin, and from the smaller fluorescence change associated with polymerization of this actin (Khaitlina et al., 1993).

The amount of F-actin subunits exchanged at any time of the reaction can be calculated using the equation derived by Brenner and Korn (1983, 1984):

$$\frac{F(t) - F(0)}{F_m(\infty) - F(0)} = \frac{C_0}{C_0 - C_c}\,(1 - e^{-X/C_c})$$

Where $F(0)$ is the fluorescence of labeled G-actin; $F(t)$ and $F_m(\infty)$ are the fluorescence signals at time t and at the final equilibrium, respectively; C_0 and C_c are the total actin concentration and critical monomer concentration, respectively; and X is the amount of F-actin subunits exchanged at time t. With C_c values determined in parallel experiments, 0.11 μM for intact and 3.0 μM for cleaved actin (see next section), the amount of F-actin subunits exchanged with the monomer pool at the time when the fluorescence plateau was reached was calculated to be 0.09 μM for intact and

TABLE 1 Rates of the steady-state ATP hydrolysis and monomer-polymer subunit exchange on intact and ECP cleaved F-actin

	ATPase Activity(mol/mol actin/h)		Initial Rate of Subunit Exchange (mol/mol/actin/h)	
Actin	Measured	Normalized to the same N	Measured	Normalized to the same N
Intact	0.038 ± 0.005 (6)	0.038	0.112 ± 0.010 (3)	0.112
Cleaved	4.31 ± 0.10 (9)	1.4–2.7	5.85 ± 0.25 (4)	1.9–3.7

The data are means ± SEM from the number of determinations given in the parentheses. The initial rates of monomer-polymer subunit exchange were calculated as described in the text. N denotes the number concentration of the filaments in the solutions of the two F-actins.

3.91 μM for cleaved actin. These amounts correspond to only 0.8% of F-actin subunits of intact, and as much as 44% of subunits of ECP modified F-actin.

Table 1 compares the initial exchange rates, expressed as moles of monomer exchanged/mol of total actin/h, with the steady-state ATP hydrolysis rates. This comparison shows that, under conditions of our experiments, the rates of the polymer subunit exchange were higher than those of ATP hydrolysis, especially in solutions of intact actin. This difference seems to reflect a contribution of an exchange of ATP-monomers with ATP-actin protomers to the overall exchange rate, consistent with there being a cap of ATP carrying subunits at least at one, the fast-growing (barbed) end of the filament (for a review see Carlier, 1989). Table 1 also shows that cleavage of actin between residues 42 and 43 increased the rates of the monomer-polymer subunit exchange and ATP hydrolysis by two or nearly two orders of magnitude. Part of this effect might, however, result from a difference in the number concentration of filament ends in solutions of intact and cleaved F-actin. To correct for this factor we have determined relative number concentrations of filaments in solutions of these actins under conditions used in the monomer-polymer subunit exchange experiments. This was accomplished by measuring their ability to nucleate polymerization when diluted into solutions of a single G-actin species above its critical concentration in polymerizing buffer (see Materials and Methods).

The initial rates of polymer growth on 0.5 μM seeds obtained from KCl-polymerized 12 μM Mg-F-actins indicated a higher number concentration of polymerization-competent filament ends in ECP-cleaved F-actin solutions than in those of intact F-actin by a factor varying from 1.6 up to 3.1 for various pairs of F-actin preparations (data from measurements on 10 different preparations). This result is consistent with the lower mechanical stability of filaments of the cleaved actin (Khaitlina et al., 1993).

Precise determination of the relative number concentrations of filaments in F-actin solutions used in the polymer subunit exchange experiments does not seem to be possible because of the difference in the procedures involved in these two kinds of measurements. In particular, the pipetting of concentrated F-actin solutions into G-actin is more likely to cause filament fragmentation than their gentle mixing with a small amount of G-actin in the exchange experiments. Therefore, instead of average values, in Table 1 we indicate the range of the rates of ATP hydrolysis and polymer subunit exchange in ECP-modified F-actin normalized to the number of filaments in solutions of intact F-actin with the normalization factors from 1.6 to 3.1. From these data it appears that ECP cleavage results in a 17-fold to 33-fold acceleration of the polymer subunit exchange, and 34-fold to 71-fold increase in the ATPase rate.

Association of actin monomers carrying ATP with one of the filament ends, and dissociation of the filament subunits carrying ADP from the other end, generating a flux of subunits from one filament end to the other (treadmilling), was the first mechanism proposed to explain the turnover of actin monomers in F-actin solutions at steady state (Wegner, 1976). Further studies pointed to the possibility of diffusional exchange of monomers at the two ends by random fluctuations in the polymer lengths (Wegner and Neuhaus, 1981; Brenner and Korn, 1983). The relative contribution of these mechanisms can be determined by kinetic analysis of incorporation of labeled monomers into the polymer at steady state. The treadmilling model predicts a linear dependence of the term $-\ln[F(\infty) - F(t)]$ on the time (t), whereas in the diffusional exchange model this term is linear with $t^{1/2}$ (Brenner and Korn, 1983). As one can see in Fig. 4, our data for both intact and cleaved actin are more consistent with the diffusional exchange mechanism than with treadmilling, although the preponderance of the diffusional exchange was not large. For intact actin, the fit to this model was good for the initial 49% of the total increase in the fluorescence, but up to 42% was also consistent with treadmilling. The fluorescence data for cleaved actin fit the linear dependence on $t^{1/2}$ up to 94% of the final increase, but for the time to reach 84% of the final fluorescence enhancement the data equally well fit the theoretical curve for the treadmilling mechanism. In general, our results are consistent with the dependence of the exchange mechanism on ionic composition of the medium (Wegner and Neuhaus, 1981; Brenner and Korn, 1983).

Effects of ECP cleavage on the rate constants of the monomer-polymer end interactions. Implications for the steady-state monomer-polymer subunit exchange

To evaluate the effects of ECP cleavage on the rate constants for the monomer addition to and dissociation from the filament

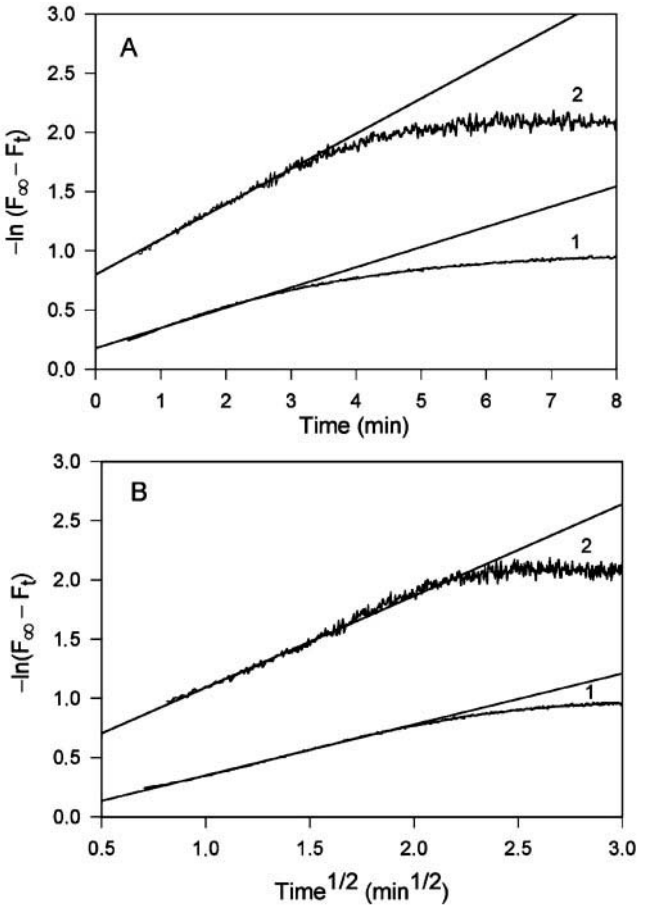

FIGUR E 4 Analysis of the kinetics of steady-state monomer-polymer subunit exchange. The fluorescence data in Fig. 3 are replotted according to the treadmill model (*A*) or to the exchange-diffusion model (*B*) as described in the text. *Curves 1* are for intact, and *2* for ECP-cleaved actin. The straight lines drawn through the initial parts of the traces show the theoretical linear dependence of $-\ln(F_\infty - F_t)$ on time or time$^{1/2}$ predicted by treadmill model and by exchange-diffusion model, respectively.

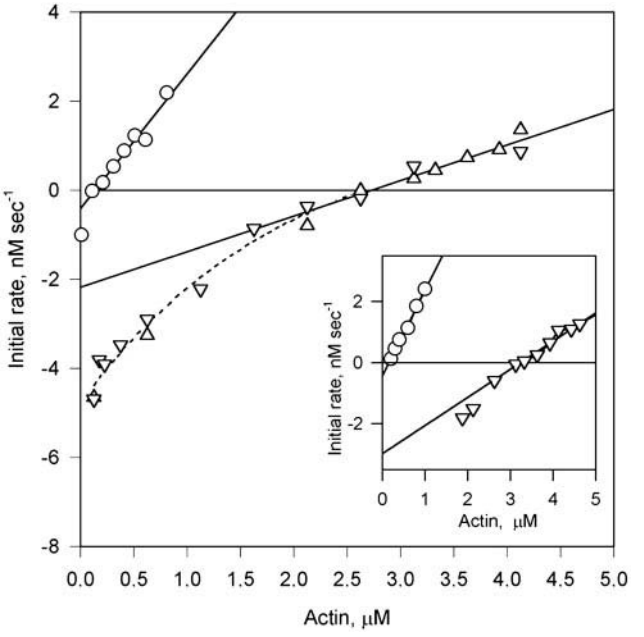

FIGUR E 5 Rates of filament elongation or depolymerization as a function of the monomer concentration. Solutions of 9% pyrenyl-labeled intact (*circles*) or ECP-cleaved Mg-G-actin (*triangles*) were supplemented with 0.1 M KCl several seconds before addition of F-actin seeds at the final concentration of 0.5 μM. The seeds were prepared from the same stock solutions of pyrenyl-labeled Mg-G-actins, intact or ECP-cleaved, respectively. The initial rates of filament elongation (at monomer concentrations above C_c) or depolymerization (below C_c) were measured as described in Materials and Methods. The data for ECP actin, normalized to the number concentration of filaments in the F-actin seed solutions of intact actin, are from two independent experiments. Most of the points for intact actin from these experiments superimposed, therefore the data from only one of these experiments are illustrated. The *inset* shows the data for intact and ECP-cleaved actin both polymerized on the cleaved F-actin seeds.

ends, we have examined the G-actin concentration dependence of the initial rates of nucleated (seeded) polymerization of the cleaved and intact pyrenyl-labeled G-actin (Pollard, 1983). The initial rates of depolymerization of F-actin seeds at G-actin concentrations below the critical concentration for polymerization were also measured. For comparison with data from the monomer-polymer subunit exchange experiments, the same polymerization conditions were used.

Fig. 5 shows the results obtained with F-actin seeds homologous to the polymerizing G-actin species, cleaved or intact, after normalization to the same number concentration of seeds. The initial G-actin concentrations include monomeric actin introduced with the F-actin seeds (calculated from the critical concentration). In agreement with earlier observations on intact actin in the presence of ATP (Carlier et al., 1986), the plot of the initial rates versus monomer concentration for cleaved actin exhibited a downward bend below the critical concentration. The slopes of the positive branches of the curves are proportional to the rate constants for addition of ATP-G-actins to polymer ends (k_+). From the data in Fig. 5 and other experiments of this kind it appears that k_+ for cleaved actin is threefold lower than that for an intact one. Since this factor critically depends on the accuracy of determination of the relative number concentration of the filament ends in F-actin seed preparations, it was important to find that the same factor of 3 was obtained when polymerization of the two actins was initiated by the same seed preparation (see the inset to Fig. 5). The C_c value of 3.0 $\pm$ 0.1 μM (average $\pm$ SD from four measurements) for the cleaved actin, obtained as an intercept at the abscissa, is in good agreement with the value earlier obtained from steady-state measurements (Khaitlina et al., 1993). It is ~30-fold higher than the value obtained here for intact actin (0.11 $\pm$ 0.01 μM). Extrapolation of the positive, linear branches of the curves to the monomer concentration $c = 0$ (intercepts at the ordinate) yields relative rate constants for dissociation of ATP-G-actin subunits from the filaments. This constant was found to be about ninefold higher for cleaved actin. The actual ordinate intercept obtained from

measurements of initial depolymerization rates was shown to correspond to the dissociation rate of ADP-G-actin subunits from the polymer (Carlier et al., 1984). The relative rate constant of this reaction in both intact and cleaved actin was two-to-threefold higher than the extrapolated value, in good agreement with the ratio of k_- values derived by others from polymerization kinetics of intact ATP-Mg-G-actin and ADP-Mg-G-actin in KCl (Pollard, 1986; Gershman et al., 1989). ECP cleavage of actin enhanced this rate constant by a factor of 5 or more, as the course of the negative branch of the plot for cleaved actin suggests further bending of the curve at monomer concentrations below 12.5 nM, the lowest that could be attained because of the high C_c value for this actin.

Independent of the mechanism of the polymer subunit exchange at steady state (treadmilling or diffusional exchange at both ends), it is the rate of subunit dissociation from the polymer ends that determines the rate of monomer association to maintain steady state (for a review see Carlier, 1989). From the data presented in this section it appears that the major effect of ECP cleavage is on the rate constant for dissociation of ATP-subunits. One can expect a similar effect on k_- for subunits carrying ADP-P_i, a transient in ATP hydrolysis on the polymer, because this state is kinetically (for a review see Carlier, 1989) and structurally (Orlova and Egelman, 1992; Muhlrad et al., 1994) similar to ATP-subunits. The enhancement of k_- for the terminal ATP- and ADP-P_i-subunits, along with the lowering of k_+ for ATP-G-actin, destabilize the barbed end of the filament, facilitating temporal exposure of ADP-subunits that dissociate fast. This explains the enhancement of subunit exchange through the diffusional exchange mechanism.

The relative values of k_- for ADP-subunits, obtained as the ordinate intercepts of F-actin depolymerization curves, represent average values for both filament ends. Thus, the enhancement of this constant by ECP-cleavage explains the acceleration of both the diffusional exchange at both ends, and treadmilling that is driven by dissociation of ADP-subunits from the pointed end. It is also consistent with and explains the larger enhancement of the rate of steady-state ATPase, resulting from exchange of ADP-subunits for ATP-monomers, than that of the overall rate of exchange (Table 1).

Effects of phalloidin on the steady-state ATP hydrolysis in solutions of ECP-cleaved F-actin

Phalloidin is known to stabilize actin filaments and reduce actin critical concentration by diminishing the rate constants of F-actin subunit dissociation from both ends of the filament (Estes et al., 1981; Coluccio and Tilney, 1984). We have previously shown that this toxin stabilizes filaments assembled from ECP cleaved Mg-G-actin against disruptive effects of centrifugal forces and shear stress (Khaitlina et al., 1993). As shown in Fig. 6, phalloidin nearly completely inhibited the steady-state ATP hydrolysis by ECP-cleaved Mg-F-actin when added to it at a 1:1 molar ratio. This confirms that the enhanced ATPase activity of the cleaved F-actin results from the increased rate of the monomer dissociation/association events. Fig. 6 also shows that the effect of phalloidin was cooperative: a half-maximal inhibition of the hydrolysis was reached at phalloidin-to-actin molar ratio of ~1:8.

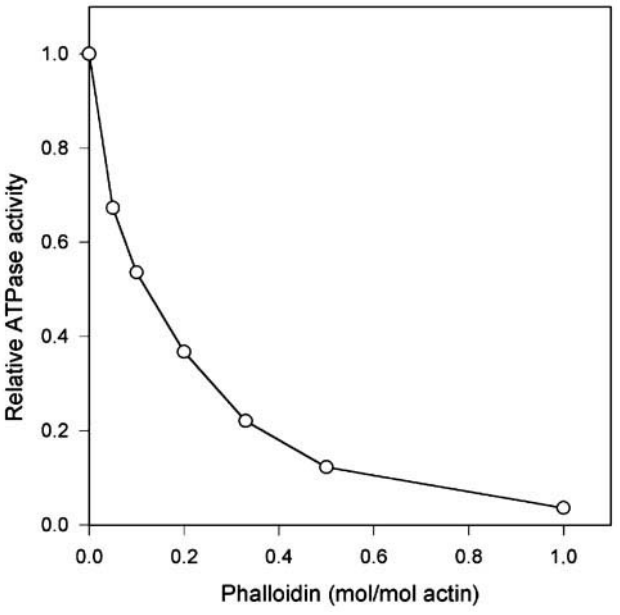

FIGURE 6 Effect of phalloidin on ATP hydrolysis by ECP-cleaved F-actin at steady state. Samples of ECP-cleaved Mg-G-actin (24 μM) were polymerized with 0.1 M KCl for 30 min at 25°C in the presence of various concentrations of phalloidin, and the F-actins were further incubated at 25°C. At time intervals, aliquots were withdrawn for P_i determination. The ATPase activity was calculated from linear plots of the amounts of P_i liberated versus time.

Further down we present data on changes in the monomer and polymer structure that seem to be relevant to the enhancement of the filament dynamics upon ECP cleavage of actin.

Probing the effects of ECP cleavage on G-actin structure by measuring the kinetics of exchange of the bound nucleotide

Earlier studies revealed that cleavage of actin within the DNase-I-binding loop results in increased accessibility of specific sites of trypsin cleavage at or near the interdomain cleft in G-actin (Strzelecka-Gołaszewska et al., 1993). These data have been interpreted as indicating that the cleft in the modified G-actin is more open than in intact G-actin. Here we further examined this possibility by measuring the rates of exchange of G-actin-bound ATP with free ATP in solution. It is generally believed that faster exchange reflects a wider opening of the cleft where the nucleotide is bound.

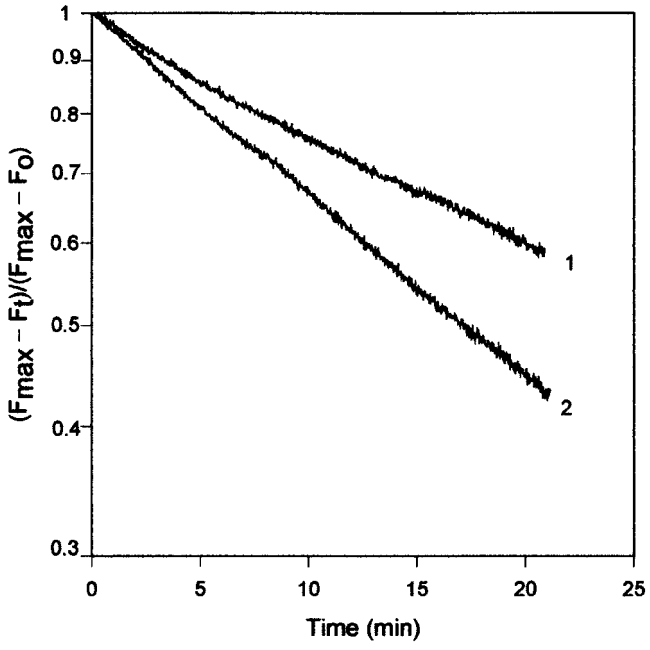

FIGURE 7 Time courses of exchange of bound ATP of intact and ECP-cleaved Mg-G-actins with ϵ-ATP. The exchange reaction was followed by recording the increase in ϵ-ATP fluorescence after addition of 100 μM ϵ-ATP to 4.8 μM intact (*curve 1*) or ECP-cleaved Mg-G-actin (*curve 2*) in the presence of 0.2 mM EGTA, 0.1 mM $MgCl_2$, and 0.8–1.2 μM free ATP, at 25°C. F_{max} is the fluorescence intensity at equilibrium, F_t is the fluorescence intensity at time t, and F_0 is the fluorescence intensity of ϵ-ATP alone.

Fig. 7 shows replacement of bound ATP with its analog etheno-ATP, monitored by recording the increase in the fluorescence intensity of etheno-ATP upon its binding to actin (Miki et al., 1974), as a function of time. The data are presented in the form of a semilogarithmic plot according to the first-order rate equation describing the unimolecular exchange reaction (Kuehl and Gergely, 1969). The apparent rate constants of the exchange, obtained from the slopes of the lines fitting the fluorescence traces, were 4.0×10^{-4} s^{-1} for intact and 7.3×10^{-4} s^{-1} for ECP-cleaved actin (average values from measurements on two different actin preparations).

Earlier measurements of the rate of ATP exchange in Mg-G-actin as a function of free Mg^{2+} concentration revealed that the rate drops down to a constant (minimum) value at $MgCl_2$ concentrations above 60 μM (Strzelecka-Gołaszewska, 1973). Since our present measurements were done in the presence of 100 μM $MgCl_2$, the obtained values represent limiting values for ATP release from G-actin with the high-affinity site for divalent cation saturated with Mg^{2+}. The nearly twofold higher value for cleaved actin than for intact actin confirms that this modification changes the monomer conformation into a more open one.

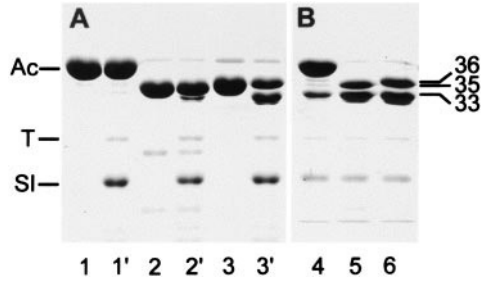

FIGURE 8 Trypsin digestion of intact, subtilisin-cleaved, and ECP-cleaved Mg-actins. (*A*) Mg-F-actins (24 μM, polymerized with 0.1 M KCl for 30 min at 25°C) were digested with trypsin at an enzyme/protein mass ratio of 1:5 for 5 min at 25°C. Electrophoretic patterns of nonmodified (*lanes 1*, *1′*), subtilisin-modified (*lanes 2*, *2′*), and ECP-modified actins (*lanes 3*, *3′*) before and after digestion with trypsin, respectively, are shown. (*B*) Electrophoretic patterns of 12 μM nonmodified (*lane 4*), subtilisin-modified (*lane 5*), and ECP-modified Mg-G-actin (*lane 6*) digested with trypsin in the monomer form at an enzyme/protein mass ratio of 1:20 for 5 min at 25°C. Positions of actin (*Ac*), its C-terminal fragments produced by subtilisin (35 kDa) and by ECP (36 kDa), the 33-kDa product of trypsin cleavage at Arg-62, trypsin (T), and soybean trypsin inhibitor (SI) are indicated.

Probing the structure of proteolytically modified F-actins by limited digestion with trypsin

After polymerization of either Ca- or Mg-G-actin with 0.1 M KCl, the specific sites of trypsin cleavage at Arg-62 and at Lys-68 in subdomain 2 of actin (Jacobson and Rosenbusch, 1976) become virtually inaccessible for the enzyme (Strzelecka-Gołaszewska et al., 1996). As shown in Fig. 8 *A*, F-actin assembled from subtilisin-cleaved Mg-G-actin was also fairly resistant to trypsin: only a small fraction of the 35-kDa product of subtilisin cleavage (residues 48–375) was degraded to the 33-kDa fragment, the product of trypsin cleavage at Lys-68. In contrast, F-actin assembled from ECP-cleaved Mg-G-actin was easily fragmented by trypsin (Fig. 8 *A*, *lanes 3* and *3′*). Such a difference between subtilisin and ECP-cleaved actins was not observed when these actins were digested in the monomer form. As shown in Fig. 8 *B*, both modifications increased the susceptibility of trypsin cleavage sites in subdomain 2 of the monomer to a similar extent.

In view of the relatively high critical concentration of ECP-modified actin, one might suppose that the fast digestion of the monomers coexisting with F-actin drives depolymerization of the filaments, thus providing the substrate for further digestion, whereas the filament subunits are not susceptible to trypsin. The increased dynamics of the filaments of ECP-modified actin also ensures a continuous supply of ADP-monomers that might be attacked by trypsin before the exchange of their ADP for ATP enables them to reassociate with the filament ends. Two lines of evidence argue against such a scheme as the main route of tryptic cleavage of the modified F-actin. 1) The digestion of the modified F-actin resulted in accumulation of the 33-kDa C-terminal product of specific cleavage at Lys-68

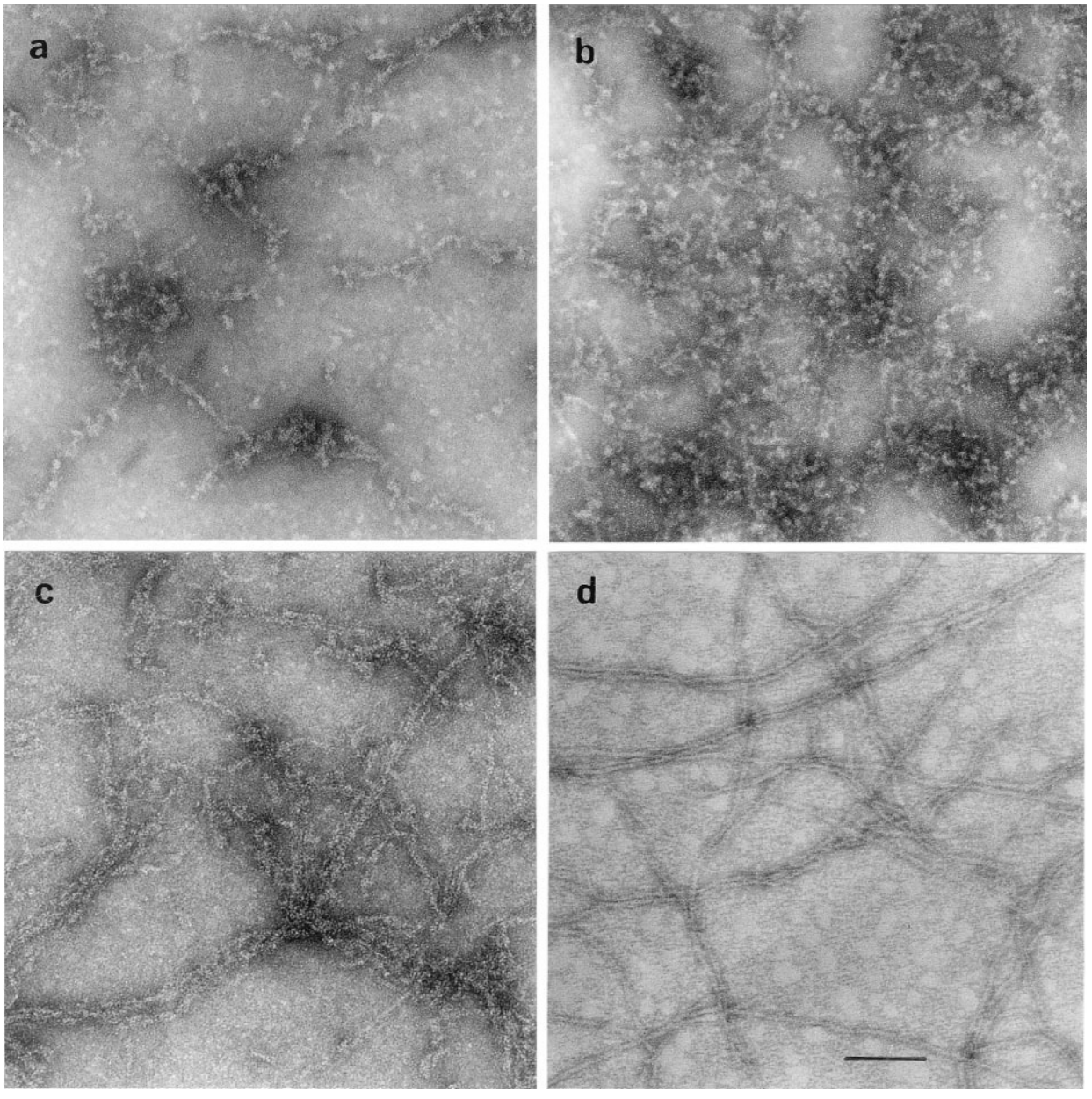

FIGURE 9 Electron micrographs of trypsin-treated filaments of ECP-cleaved and intact F-actin. Twenty-four μM ECP-cleaved (*a*, *b*) or intact Mg-G-actin (*c*) were polymerized with 0.1 M KCl and then subjected to digestion with trypsin as described in the legend to Fig. 8. After stopping the reaction with SBTI, samples of the solutions were negatively stained as described in Materials and Methods. (*d*) The filaments of ECP-cleaved F-actin digested with trypsin in the presence of equimolar phalloidin. Bar = 200 nm.

(Fig. 8 *A*, *lane 3′*). When this actin was subjected to tryptic digestion under the same conditions (0.1 M KCl, high trypsin concentration) at or below the critical concentration, the 33-kDa intermediate was fast-degraded to low molecular mass products (results not shown). 2) The second comes from inspection of the digests in the electron microscope. It is known that trypsin cleaved G-actin is unable to polymerize (Jacobson and Rosenbusch, 1976). Therefore, if the trypsin cleavage sites in subdomain 2 in ECP-modified F-actin were inaccessible to this enzyme, the filaments seen in negatively stained preparations of partially digested ECP-modified F-actin should be morphologically indistinguishable from those of trypsin-treated non-modified F-actin. This was not the case. Electron micrographs of ECP-modified actin fragmented by trypsin in ~70% showed the presence of abundant filamentous material. However, all filaments seen on the grids, like those in Fig. 9 *a*, were highly disordered. They appeared extremely flexible, associated with short filament fragments, and frequently entangled into large irregular aggregates. A fragment of such an aggregate is shown in Fig. 9 *b*. Most probably these were joint

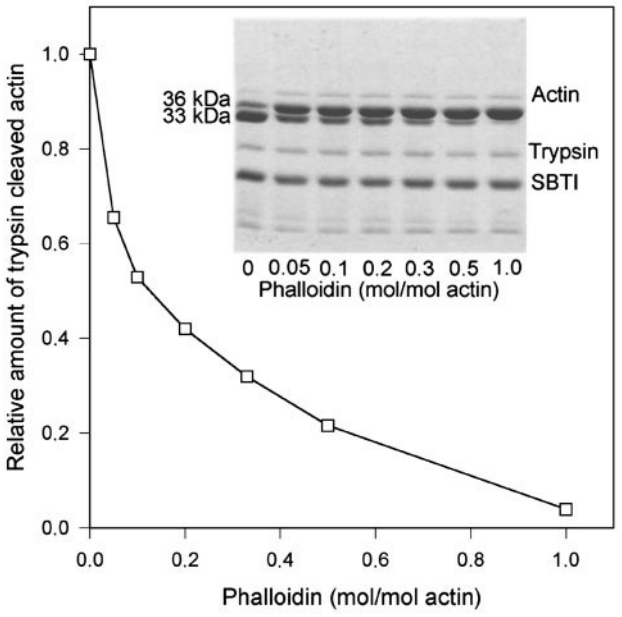

FIGURE 10 Effect of phalloidin on the susceptibility of subdomain 2 in ECP-cleaved F-actin to tryptic digestion. ECP-cleaved Mg-G-actin (24 μM) was polymerized with 0.1 M KCl (30 min at 25°C) in the presence of phalloidin at molar ratios to actin as indicated in the figure. The F-actins were digested with trypsin at a trypsin/actin mass ratio of 1:5 for 5 min at 25°C. The digestions were stopped with a threefold excess of soybean trypsin inhibitor (SBTI). The digests were analyzed by SDS-PAGE (*inset*), and the relative intensities of the 36-kDa C-terminal product of ECP cleavage of actin were measured as described in Materials and Methods. Positions of the 36-kDa fragment produced by ECP cleavage and of the 33-kDa product of its trypsin cleavage are indicated in the inset.

effects of the cleavages at Arg-62 and Lys-68 in subdomain 2 of actin and of the removal by trypsin of the two or three C-terminal residues (O'Donoghue et al., 1992; Mossakowska et al., 1993). However, the C-terminal truncation alone does not cause such dramatic changes in the filament structure. In agreement with O'Donoghue et al. (1992), trypsin treatment of the filaments of intact actin, producing no significant cleavage at the sites in subdomain 2 (Fig. 8 *A*, *lane 2*), increased flexibility of the filaments and promoted their fragmentation and bundling (Fig. 9 *c*), but the extent of disorder was less than observed with similarly treated ECP modified F-actin.

From the above-described observations one can conclude that in KCl-polymerized ECP-modified Mg-actin, the sites of trypsin cleavage in subdomain 2 are or become transiently exposed upon thermal fluctuations of the filament structure.

Fig. 9 *d* shows the filaments of ECP-modified F-actin treated with trypsin in the presence of phalloidin equimolar to actin. Morphologically, these filaments were indistinguishable from those of the modified F-actin without phalloidin but not subjected to trypsin digestion (not shown). The stabilization by phalloidin of the polymer structure is consistent with SDS-PAGE analysis showing nearly complete protection of actin from tryptic cleavage under these conditions (Fig. 10, *inset*, *lane 1.0*). As can be seen in Fig. 10, this effect of phalloidin was cooperative. Comparison with data in Fig. 6 shows that the dependence of the protection of the trypsin cleavage sites in subdomain 2 on the phalloidin-to-actin ratio remarkably well-matched the dependence of the inhibition by phalloidin of the steady-state ATPase activity of ECP-modified F-actin. In both cases the half-maximal change was observed at a phalloidin-to-actin molar ratio of ~1:8. This correlation strongly suggests that the changes in the filament structure revealed by limited proteolysis with trypsin significantly contribute to the increased dynamics of the filaments of ECP modified actin.

DISCUSSION

Previous studies have shown that actin cleaved with ECP between Gly-42 and Val-43 does not polymerize if its high-affinity site for divalent cation is occupied by Ca^{2+}, and that its Mg^{2+}-bound form has higher critical concentration and polymerizes more slowly than Mg-G-actin cleaved with subtilisin between Met-47 and Gly-48 (Khaitlina et al., 1991, 1993). Here we show that the cleavage with ECP diminishes the rate constant for addition of ATP-G-actin to the polymer ends and increases the rate constant for dissociation of newly incorporated ATP-subunits (and, presumably, ADP-P_i-subunits). Determination of the rates of F-actin depolymerization as a function of the monomer concentration indicated a substantial increase also in the rate constant for dissociation of ADP-subunits. The increase in the rates of subunit dissociation resulted in the enhancement of the rate of subunit exchange in Mg-F-actin by at least an order of magnitude. In contrast, as judged from the measurements of the F-actin ATPase activity, the cleavage with subtilisin has a relatively small effect on the polymer subunit turnover.

These observations are consistent with the prediction of the atomic models of F-actin that the N-terminal segment of loop 39–51 directly participates in the intermolecular interactions in the filament and emphasize the role of this contact in stabilization of the filament. However, in addition to the direct effect on the putative monomer-monomer interface, cleavage of actin between Gly-42 and Val-43 generates changes in the conformation of other areas of the molecule (Strzelecka-Gołaszewska et al., 1993; Khaitlina et al., 1996; Kuznetsova et al., 1996) which might contribute to the deficient polymerizability of the modified actin and instability of its filaments. In this respect, the most important seems to be the change in the overall conformation of subdomain 2 as revealed by limited digestion with trypsin.

Crystallographic investigations of β-actin/profilin complexes provided a direct evidence that G-actin can adopt either an open or tight (closed) conformation by a hinged rotation of subdomain 2 (Chik et al., 1996). The refined models of muscle F-actin predict that the polymer subunits assume a tight conformation that is necessary to increase the number of potential intermonomer contacts involving the DNase-I-binding loop (Lorenz et al., 1993; Tirion et al., 1995). The relationship between the filament stability and

orientation of subdomain 2 has also been suggested based on electron microscopic three-dimensional reconstructions of yeast F-actin, exhibiting high steady-state ATPase activity, and its mutants in which this ATPase is suppressed (Chen and Rubenstein, 1995; Orlova et al., 1997; Belmont et al., 1999). Transition of monomeric actin from open to tight conformation upon treatments that initiate polymerization (addition of salt) or accelerate it (exchange of actin-bound Ca^{2+} for Mg^{2+}) is suggested by diminished accessibility of tryptic cleavage sites in subdomain 2, on a side of the interdomain cleft (Khaitlina et al., 1996; Strzelecka-Gołaszewska et al., 1993, 1996; Strzelecka-Gołaszewska, 2000). An opposite change, i.e., the facilitation of trypsin cleavage, as well as the enhanced rate of nucleotide exchange, indicate that proteolytic cleavage of actin within the DNase-I-binding loop shifts the equilibrium between the G-actin states toward a more open one.

At first sight, the relevance of this change to polymerization may seem to be contradicted by virtually the same effect of ECP and of subtilisin cleavage on the monomer structure. However, this is what should be expected if, as it has been shown, in monomeric actin with ATP as the bound nucleotide the entire loop is unrestrained and able to freely fluctuate (McLaughlin et al., 1993; Suda and Saito, 1994). The differences in structure reveal itself after polymerization. As indicated again by limited digestion with trypsin, the transition from tight to open conformation induced by cleavage with ECP is not, or not entirely, reversed by polymerization, whereas F-actin assembled from subtilisin-cleaved monomers more closely resembles intact F-actin than ECP-cleaved. In this context, it is interesting to note a similarity between ECP-cleaved muscle α-actin and yeast actin in both the increased dynamics of their filaments, correlating with a wider opening of the interdomain cleft (Orlova et al., 1997; Belmont et al., 1999), and the requirement of the presence of Mg^{2+} at the high-affinity site for divalent cation to undergo KCl-induced polymerization (Khaitlina et al., 1993; Kim et al., 1996). The effect of Mg^{2+} may be connected with its stimulation of the monomer transition from open to the F-actin-like closed state.

These observations suggest that the destabilization of actin filaments by ECP cleavage is, at least in part, due to an intramolecular effect of this modification on the relative orientation of subdomain 2. They also argue for distinct roles of various parts of loop 39–51 in the monomer-monomer interactions, supporting the prediction of Holmes et al. and Lorenz et al. models that residues 42 and 43 are at the monomer-monomer interface, whereas the outer part of the loop (encompassing the subtilisin cleavage site) is beyond it. In terms of this model, cleavage of the N-terminal segment of the loop can be expected to weaken the interactions that stabilize the closed conformation of the polymer subunits in intact F-actin, whereas the conformational defects of subtilisin-cleaved actin can be corrected for by polymerization because, in this actin, the N-terminal segment of the loop is still functional.

Location of the C-terminal segment of loop 39–51 close to but not at the monomer-monomer interface is also consistent with the reported restriction of thermal bending motions in the filaments of subtilisin-cleaved actin (Isambert et al., 1995; Borovikov et al., 2000). This apparently puzzling effect suggests that, in non-modified F-actin, thermal motions of the unrestrained C-terminal segment of the loop contribute to the filament flexibility by causing temporal deformations of the monomer-monomer interface involving the N-terminal segment. Subtilisin cleavage interrupts the transmission of these motions to the N-terminal segment of the loop and thus stabilizes its contacts. This effect of subtilisin cleavage, albeit smaller than that reported for phalloidin-free filaments (Isambert et al., 1995), has also been observed with filaments labeled with rhodamine-phalloidin (Borovikov et al., 2000), in agreement with the x-ray diffraction data showing that phalloidin restricts but does not eliminate the mobility of loop 39–51 in F-actin (Lorenz et al., 1993).

Presently available evidence from electron microscopic (Orlova and Egelman, 1992; Belmont et al., 1999) and biochemical data (Muhlrad et al., 1994; Moraczewska et al., 1999) suggests that destabilization of F-actin by the release of P_i following ATP hydrolysis on the polymer is mediated by concerted changes in the interdomain relations (opening of the interdomain cleft) and in the arrangement of loop 39–51. This sequence is consistent with a putative "back-door" mechanism of P_i release (Wriggers and Schulten, 1999). It does not, however, exclude the possibility that actin modifications generating a relatively more open conformation of the ADP-P_i-subunits of the polymer facilitate P_i release through the interdomain cleft, and thus accelerate it. Such a mechanism might operate in ECP-cleaved F-actin and contribute to the acceleration of the subunit exchange by diminishing the protective cap of ADP-P_i-subunits. Verification of this hypothesis is our future experimental goal.

Enhancement of the polymer subunit turnover has earlier been observed upon various modifications of the C-terminal segment of actin (Drewes and Faulstich, 1990, 1993; Mossakowska et al., 1993). The effects of these modifications were far less pronounced than the effect of cleavage with ECP. This is consistent with more extensive inter-monomer interactions of loop 39–51, as predicted from the F-actin models, and with their crucial role in stabilization/destabilization of the F-actin structure. Another difference between the effects of these modifications is revealed by comparison of their cooperative reversal by phalloidin. The half-maximal protection of ECP-cleaved actin required one phalloidin molecule per eight actin molecules, whereas with C-terminally modified actins it was afforded at one phalloidin per 20 actins (Drewes and Faulstich, 1990, 1993). This difference is not due to possible differences in the affinity of this toxin to the modified actins because complete protection was observed at the same 1:1 molar ratio of phalloidin

to actin. A mechanism of stabilization different than cooperative restoration of stable conformation of the filament subunits, e.g., a blocking the filament ends by a small number of phalloidin-actin complexes, is excluded by our tryptic digestion experiments showing that the inhibition of subunit exchange paralleled the changes in structure of the polymer subunits. A similar conclusion with regard to C-terminally modified actin has been derived from analysis of three-dimensional reconstructions of phalloidin-treated filaments (Orlova et al., 1995). The reduced cooperativity of the response of ECP-cleaved actin to phalloidin binding points to the important role of loop 39–51 in transmission of cooperative effects along the filament.

Our analysis of the mechanism of monomer-polymer subunit exchange shows that the diffusional exchange at both filament ends and treadmilling can efficiently operate in filaments more dynamic than those of skeletal muscle α-actin. In non-muscle cells the directionality and rate of the polymer subunit turnover are temporally and spatially regulated by various actin-binding proteins and membrane-linked signaling (Carlier, 1998; Chen et al., 2000). The results of the present work show that allosteric effects on the conformation of the N-terminal part of the DNase-I-binding loop that have already been observed with several actin-binding proteins (for a review see Khaitlina, 2001) might be a powerful tool in this regulation.

We are grateful to Drs. Alevtina Morozova and Alexander Malinin for their generous gift of purified protease ECP32. We also thank Barbara Wawro for pyrenyl-labeled actin, Emilia Karczewska for the excellent technical assistance, and Dr. Natalia Kulikova for the help in preparing the graphs.

This work was supported by Grant 6 P04A 01417 (to H.S-G.) and a grant to the Nencki Institute from the State Committee for Scientific Research (Poland); and by Grant 99-04-49482 (to S.Yu.Kh.) from the Russian Foundation for Basic Research.

REFERENCES

Asakura, S., and F. Oosawa. 1960. Dephosphorylation of adenosine triphosphate in actin solutions at low concentrations of magnesium. *Arch. Biochem. Biophys.* 87:273–280.

Belmont., L. D., A. Orlova, D. G. Drubin, and E. H. Egelman. 1999. A change in actin conformation associated with filament instability after P_i release. *Proc. Natl. Acad. Sci. U.S.A.* 96:29–34.

Ben-Avraham, D., and M. M. Tirion. 1995. Dynamic and elastic properties of F-actin: a normal-mode analysis. *Biophys. J.* 68:1231–1245.

Borovikov, Yu. S., J. Moraczewska, M. I. Khoroshev, and H. Strzelecka-Gołaszewska. 2000. Proteolytic cleavage of actin within the DNase-I-binding loop changes the conformation of F-actin and its sensitivity to myosin binding. *Biochim. Biophys. Acta.* 1478:138–151.

Brenner, S. L., and E. D. Korn. 1981. Stimulation of actin ATPase activity by cytochalasins provides evidence for a new species of monomeric actin. *J. Biol. Chem.* 256:8663–8670.

Brenner, S. L., and E. D. Korn. 1983. On the mechanism of actin monomer-polymer subunit exchange at steady state. *J. Biol. Chem.* 258: 5013–5020.

Brenner, S. L., and E. D. Korn. 1984. Evidence that F-actin can hydrolyze ATP independent of monomer-polymer end interactions. *J. Biol. Chem.* 259:1441–1446.

Byers, H. R., G. E. White, and K. Fujiwara. 1984. Organization and function of stress fibers in cells in vitro and in situ. A review. *In* Cell and Muscle Motility, Vol. 5. J. W. Shay, editor. Plenum Publishing Corporation, New York. 83–137.

Carlier, M.-F. 1989. Role of nucleotide hydrolysis in the dynamics of actin filaments and microtubules. *Int. Rev. Cytol.* 115:139–170.

Carlier, M.-F. 1998. Control of actin dynamics. *Curr. Opin. Cell Biol.* 10:45–51.

Carlier, M.-F., D. Pantaloni, and E. D. Korn. 1984. Evidence for an ATP cap at the ends of actin filaments and its regulation of the F-actin steady state. *J. Biol. Chem.* 259:9983–9986.

Carlier, M.-F., D. Pantaloni, and E. D. Korn. 1986. The effects of Mg^{2+} at the high-affinity and low-affinity sites on the polymerization of actin and associated ATP hydrolysis. *J. Biol. Chem.* 261:10785–10792.

Carlier, M.-F., D. Pantaloni, and E. D. Korn. 1987. The mechanisms of ATP hydrolysis accompanying the polymerization of Mg-actin and Ca-actin. *J. Biol. Chem.* 262:3052–3059.

Chen, H., B. W. Bernstein, and J. R. Bamburg. 2000. Regulating actin-filament dynamics in vivo. *TIBS.* 25:19–23.

Chen, X., and P. A. Rubenstein. 1995. A mutation in an ATP-binding loop of *Saccharomyces cerevisiae* actin (S14A) causes a temperature-sensitive phenotype in vivo and in vitro. *J. Biol. Chem.* 270:11406–11414.

Chik, J. K., U. Lindberg, and C. E. Schutt. 1996. The structure of an open state of β-actin at 2.65 Å resolution. *J. Mol. Biol.* 263:607–623.

Coluccio, L. M., and L. G. Tilney. 1984. Phalloidin enhances actin assembly by preventing monomer dissociation. *J. Cell Biol.* 99:529–535.

Drewes, G., and H. Faulstich. 1990. The enhanced ATPase activity of glutathione-substituted actin provides a quantitative approach to filament stabilization. *J. Biol. Chem.* 265:3017–3021.

Drewes, G., and H. Faulstich. 1993. Cooperative effects on filament stability in actin modified at the C-terminus by substitution or truncation. *Eur. J. Biochem.* 212:247–253.

Estes, J. E., L. A. Selden, and L. C. Gershman. 1981. Mechanism of action of phalloidin on the polymerization of muscle actin. *Biochemistry.* 20:708–712.

Frieden, C., and K. Patane. 1985. Differences in G-actin containing bound ATP or ADP: the Mg^{2+}-induced conformational change requires ATP. *Biochemistry.* 24:4192–4196.

Gershman, L. C., L. A. Selden, H. J. Kinosian, and J. E. Estes. 1989. Preparation and polymerization properties of monomeric ADP-actin. *Biophys. Biochim. Acta.* 995:109–115.

Hegyi, G., G. Premecz, B. Sain, and A. Muhlrad. 1974. Selective carbethoxylation of the histidine residues of actin by diethylpyrocarbonate. *Eur. J. Biochem.* 44:7–12.

Holmes, K. C., D. Popp, W. Gebhard, and W. Kabsch. 1990. Atomic model of the actin filament. *Nature.* 347:44–49.

Houk, W. T., and K. Ue. 1974. The measurement of actin concentration in solution: a comparison of methods. *Anal. Biochem.* 62:66–74.

Isambert, H., P. Venier, A. C. Maggs, A. Fattoum, R. Kassab, D. Pantaloni, and M.-F. Carlier. 1995. Flexibility of actin filaments derived from thermal fluctuations. *J. Biol. Chem.* 270:11437–11444.

Jacobson, G. R., and J. P. Rosenbusch. 1976. ATP binding to a protease-resistant core of actin. *Proc. Natl. Acad. Sci. U.S.A.* 73:2742–2746.

Jockusch, B. M., A. Füchtbauer, C. Wiegand, and B. Höner. 1986. Probing the cytoskeleton by microinjection. *In* Cell and Molecular Biology of the Cytoskeleton. J.W. Shay, editor. Plenum Publishing Corporation, New York. 1–40.

Kabsch, W., H.-G. Mannherz, D. Suck, E. F. Pai, and K. Holmes. 1990. Atomic structure of the actin:DNase I complex. *Nature.* 347:37–44.

Khaitlina, S. Yu. 2001. Functional specificity of actin isoforms. *Int. Rev. Cytol.* 202:35–98.

Khaitlina, S. Yu., J. H. Collins, I. M. Kuznetsova, V. P. Pershina, I. G. Synakevich, K. K. Turoverov, and A. M. Usmanova. 1991. Physicochemical properties of actin cleaved with bacterial protease from *E. coli* A2 strain. *FEBS Lett.* 279:49–51.

Khaitlina, S. Yu., J. Moraczewska, and H. Strzelecka-Gołaszewska. 1993. The actin/actin interactions involving the N-terminus of the DNase-I-binding loop are crucial for stabilization of the actin filament. *Eur. J. Biochem.* 218:911–920.

Khaitlina, S., B. Wawro, B. Pliszka, and H. Strzelecka-Gołaszewska. 1996. Conformational changes associated with the monomer activation step of actin polymerization. *J. Muscle Res. Cell Motil.* 17:122–123.

Kim, E., C. J. Miller, and E. Reisler. 1996. Polymerization and in vitro motility properties of yeast actin: a comparison with rabbit skeletal α-actin. *Biochemistry.* 35:16566–16572.

Kim, E., M. Motoki, K. Seguro, A. Muhlrad, and E. Reisler. 1995. Conformational changes in subdomain 2 of G-actin: fluorescence probing by dansyl ethylenediamine attached to Gln-41. *Biophys. J.* 69: 2024–2032.

Kodama, T., K. Fukui, and K. Kometani. 1986. The initial phosphate burst in ATP hydrolysis by myosin and subfragment-1 as studied by a modified Malachite Green method for determination of inorganic phosphate. *J. Biochem.* 99:1465–1472.

Kouyama, T., and K. Mihashi. 1981. Fluorimetry study of N-(1-pyrenyl)iodoacetamide-labeled F-actin. Local structural change of actin promoter both on polymerization and on binding of heavy meromyosin. *Eur. J. Biochem.* 114:33–48.

Kuehl, W. M., and J. Gergely. 1969. The kinetics of exchange of adenosine triphosphate and calcium with G-actin. *J. Biol. Chem.* 244:4720–4729.

Kuznetsova, I., O. Antropova, K. Turoverov, and S. Khaitlina. 1996. Conformational changes in subdomain 1 of actin induced by proteolytic cleavage within the DNase-I-binding loop: energy transfer from tryptophan to AEDANS. *FEBS Lett.* 383:105–108.

Laemmli, U. K. 1970. Cleavage of structural proteins during the assembly of the head of bacteriophage T4. *Nature.* 227:680–685.

Lasa, I., P. Dehoux, and P. Cossart. 1998. Actin polymerization and bacterial movement. *Biochim. Biophys. Acta.* 1402:217–228.

Littlefield, R., and V. M. Fowler. 1998. Defining actin filament length in striated muscle. Rulers and caps or dynamic stability? *Annu. Rev. Cell Dev. Biol.* 14:487–525.

Lorenz, M., D. Popp, and K. C. Holmes. 1993. Refinement of the F-actin model against x-ray fiber diffraction data by the use of a direct mutation algorithm. *J. Mol. Biol.* 234:826–836.

McLaughlin, P. J., J. T. Gooch, H.-G. Mannherz, and A. G. Weeds. 1993. Structure of gelsolin segment 1-actin complex and the mechanism of filament severing. *Nature.* 364:685–692.

Miki, M., H. Ohnuma, and K. Mihashi. 1974. Interaction of actin with ϵ-ATP. *FEBS Lett.* 46:17–19.

Moraczewska, J., H. Strzelecka-Gołaszewska, P. D. J. Moens, and C. G. dos Remedios. 1996. Structural changes in subdomain 2 of G-actin observed by fluorescence spectroscopy. *Biochem. J.* 317:605–611.

Moraczewska, J., B. Wawro, K. Seguro, and H. Strzelecka-Gołaszewska. 1999. Divalent cation-, nucleotide-, and polymerization-dependent changes in the conformation of subdomain 2 of actin. *Biophys. J.* 77:373–385.

Morozova, A. V., I. N. Skovorodkin, S. Yu. Khaitlina, and A. Yu. Malinin. 2001. Bacterial protease ECP32 specifically cleaving actin, and its effect on cytoskeleton in vivo. *Biokhimia.* 66:105–113.

Mossakowska, M., J. Moraczewska, S. Yu. Khaitlina, and H. Strzelecka-Gołaszewska. 1993. Proteolytic removal of three C-terminal residues of actin alters the monomer-monomer interactions. *Biochem. J.* 289: 897–902.

Muhlrad, A., P. Cheung, B. C. Phan, C. Miller, and E. Reisler. 1994. Dynamic properties of actin: structural changes induced by beryllium fluoride. *J. Biol. Chem.* 269:11852–11858.

O'Donoghue, S. I., M. Miki, and C. G. dos Remedios. 1992. Removing the two C-terminal residues of actin affects the filament structure. *Arch. Biochem. Biophys.* 293:110–116.

Oosawa, F. 1983. Macromolecular assembly of actin. *In* Muscle and Nonmuscle Motility, Vol. 1. E. Stracher, editor. Academic Press, New York, London. 151–216.

Orlova, A., X. Chen, P. A. Rubenstein, and E. H. Egelman. 1997. Modulation of yeast F-actin structure by a mutation in the nucleotide-binding cleft. *J. Mol. Biol.* 271:235–243.

Orlova, A., and E. H. Egelman. 1992. Structural basis for the destabilization of F-actin by phosphate release following ATP hydrolysis. *J. Mol. Biol.* 227:1043–1053.

Orlova, A., E. Prochniewicz, and E. H. Egelman. 1995. Structural dynamics of F-actin. II. Cooperativity in structural transitions. *J. Mol. Biol.* 245:598–607.

Otterbein, L. R., P. Graceffa, and R. Dominguez. 2001. The crystal structure of uncomplexed actin in the ADP state. *Science.* 293:708–711.

Pollard, T. D. 1983. Measurement of rate constants for actin filament elongation in solution. *Anal. Biochem.* 134:406–412.

Pollard, T. D. 1986. Rate constants for the reactions of ATP- and ADP-actin with the ends of actin filaments. *J. Cell Biol.* 103:2747–2754.

Schwyter, D., M. Phillips, and E. Reisler. 1989. Subtilisin-cleaved actin: polymerization and interaction with myosin subfragment 1. *Biochemistry.* 28:5885–5895.

Secrist, J. A., J. R. Barrio, N. J. Leonard, and G. Weber. 1972. Fluorescent modification of adenine-containing coenzymes. Biological activities and spectroscopic properties. *Biochemistry.* 11:3499–3506.

Small, J. V., K. Anderson, and K. Rottner. 1996. Actin and the coordination of protrusion, attachment and retraction in cell crawling. *Biosci. Rep.* 16:351–368.

Spudich, J. A., and S. Watt. 1971. The regulation of rabbit skeletal muscle contraction. I. Biochemical studies of the interaction of the tropomyosin-troponin complex with actin and the proteolytic fragments of myosin. *J. Biol. Chem.* 246:4866–4871.

Stossel, T. P. 1993. On the crawling of animal cells. *Science.* 260: 1086–1094.

Strzelecka-Gołaszewska, H. 1973. Effect of tightly bound divalent cation on the equilibria between G-actin-bound and free ATP. *Eur. J. Biochem.* 37:434–440.

Strzelecka-Gołaszewska, H. 2000. Divalent cations, nucleotides, and actin structure. *In* Results and Problems in Cell Differentiation, Vol. 32. Molecular Interactions of Actin. C. G. dos Remedios, editor. Springer Verlag, Berlin, Heidelberg. 23–41.

Strzelecka-Gołaszewska, H., J. Moraczewska, S. Khaitlina, and M. Mossakowska. 1993. Localization of the tightly bound divalent-cation-dependent and nucleotide-dependent conformation changes in G-actin using limited proteolytic digestion. *Eur. J. Biochem.* 211:731–742.

Strzelecka-Gołaszewska, H., A. Woźniak, T. Hult, and U. Lindberg. 1996. Effects of the type of divalent cation, Ca^{2+} or Mg^{2+}, bound at the high-affinity site and of the ionic composition of the solution on the structure of F-actin. *Biochem. J.* 316:713–721.

Suda, H., and M. Saito. 1994. Molecular dynamics simulations for actin monomers in solution. *J. Theor. Biol.* 171:347–349.

Takashi, R. 1988. A novel actin label: a fluorescence probe at glutamine-41 and its consequences. *Biochemistry.* 27:938–947.

Tilney, L. G., and S. Inoue. 1982. Acrosomal reaction of *Thyone* sperm. II. The kinetics and possible mechanism of acrosomal process elongation. *J. Cell. Biol.* 93:820–827.

Tirion, M. M., D. ben-Avraham, M. Lorenz, and K. C. Holmes. 1995. Normal modes as refinement parameters for the F-actin model. *Biophys. J.* 68:5–12.

Wegner, A. 1976. Head to tail polymerization of actin. *J. Mol. Biol.* 108:139–150.

Wegner, A., and J.-M. Neuhaus. 1981. Requirement of divalent cations for fast exchange of actin monomers and actin filament subunits. *J. Mol. Biol.* 153:681–693.

Wriggers, W., and K. Schulten. 1999. Investigating a back door mechanism of actin phosphate release by steered molecular dynamics. *Proteins.* 35:262–273.